Response to Liu Mingliang

essd-2023-495

Title: Satellite-based Near-Real-Time Global Daily Terrestrial Evapotranspiration Estimates

Author(s): Lei Huang et al.

MS type: Data description paper

In the reply, the reviewers' comments are in *italics*, our response is in normal text, and quotes from the manuscript are in **blue**.

This paper claimed that the advantage of this new global ET data product is that it is near-real-time which has about one week's delay, but with a little bit better or comparable accuracies with other data products. The authors should discuss how much contribution of this one-week earlier (than other models/data products) to the community and how possible accuracies could be improved if more observations such as climate data are added and the estimation be delayed to two-weeks or even further. The authors also need make the near-real-time data public available or accessible (i.e. the data products will be updated at real time if being needed); or the source code or tool could be used to calculate global ET through cloud computing platforms, such as GEE. The bias on estimated air temperature and net radiation (might also need add some comparisons with other regional and global data sets on net radiation estimations) should be addressed before publishing this data products since the estimated air temperature and the application of shortwave radiation as input is the bases of this near-real-time ET products. What are the uncertainties coming from the estimated EF by using calculated vegetation and soil resistance, rather than directly from remote sensed information, such as surface temperature and NDVI (through Ts-VI triangle method)?

Re: We thank the reviewers! We have added discussion about contribution of the one-week earlier to the community and how possible accuracies could be improved at Lines 702-707:

"The VISEA ET product provides near-real-time global evapotranspiration (ET) data with a mere one-week delay and a daily resolution of 0.05 degrees. It empowers researchers by providing access to information on land surface water consumption in near-real-time, which is crucial for monitoring and predicting droughts, and enables decision-makers to make well-informed choices. This not only enhances research efficiency but also supports more effective and expedited actions within the scientific and environmental research community. The accuracy of the VISEA model could be enhanced by incorporating additional

satellite and climate data with higher time resolution. Moreover, the one-week delay in providing ET data could be reduced to three days or less by integrating real-time updated satellite observation data."

We have uploaded our ET data at National Tibetan Plateau Data Center Third Pole Environment Data Center at lines 746-747:

"The VISEA ET data can be obtained from https://data.tpdc.ac.cn/en/data/236e33bf-e66b-4682-bbc1-274de1dcbcd3 (Huang, 2023a)."

All the calculation codes have been uploaded at figshare website at lines 742-744:"…the codes for generating the global ET products can be obtained through the public repository at https://doi.org/10.6084/m9.figshare.24647721.v1 (Huang, 2023c)"

We have compared our estimated daily air temperature and net radiation with local measurements at Figure 4 and 5. VISEA model exclusively utilized MODIS land products and shortwave radiation data from ERA5-Land as inputs, as detailed in Table 1. We added the global shortwave radiation from Clouds and the Earth's Radiant Energy System, CERES as our VISEA model input to calculated the daily net radiation, air temperature and ET for comparison in the Supplementary Figure S1-S3. It is important to note that the observed discrepancies in temperature and radiation between remote sensing observations and measurements at various sites are characterized by diverse bias features, indicating that these biases are not systematic errors. This variability underscores the complexity of accurately estimating these parameters across different regions and highlights the importance of employing multiple data sets for validation and comparison. Our approach, including the integration of CERES data, is aimed at addressing these complexities and improving the reliability and accuracy of our near-real-time ET product estimates.

Table 1. The input of VISEA

The input of VISEA			
Data source	Data name	Used parameter	Spatial/temporal resolution
MODIS Land Product	MOD11C1	Land Surface Temperature	0.05°/ daily
	MOD09CMG	Surface Reflectance	0.05°/daily
	MCD43C3	Albedo	0.05°/daily
	MOD13C1	NDVI	0.05°/16-day
	MCD12C1	Land cover	0.05°/ yearly
ERA5-Land hourly data	Rd	Downward surface solar radiation	0.1°/ hourly

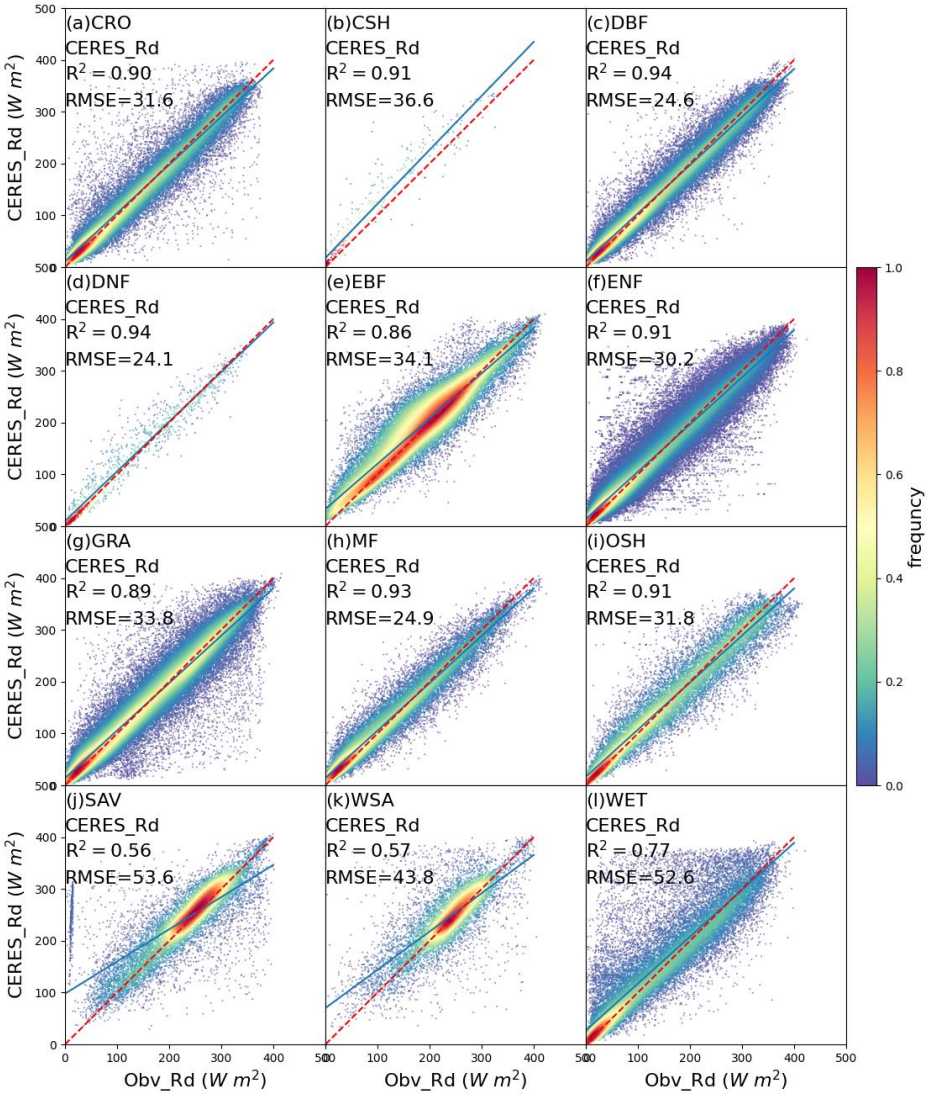

Figure S1. The scatter plot of daily downwards shortwave from Clouds and the Earth's Radiant Energy System (CERES) compared with local instruments measurements (Obv_Rd) under 12 IGBP land cover types: CRO (Croplands), CSH (Closed shrublands), DBF (Deciduous broadleaf forests), DNF (Deciduous needle leaf forests), EBF (Evergreen broadleaf forests), ENF (Evergreen needle leaf forests), GRA (Grasslands), MF (Mixed forests), OSH (Open shrublands), SAV (Savannas), WSA (Woody savannas), WET (Permanent wetlands). The red dotted line is the 1:1 line. N is the number of data points, NSE is Nash-Sutcliffe Efficiency, R is correlation coefficients, RMSE is Root Mean Square Error, RMSEs is systematic RMSE, and RMSEu is unsystematic RMSE. The frequency denotes the probability density estimated through the Kernel Density Estimation, KDE method with a Gaussian kernel, and it is then scaled to ensure that the maximum value of the probability density function equals 1.

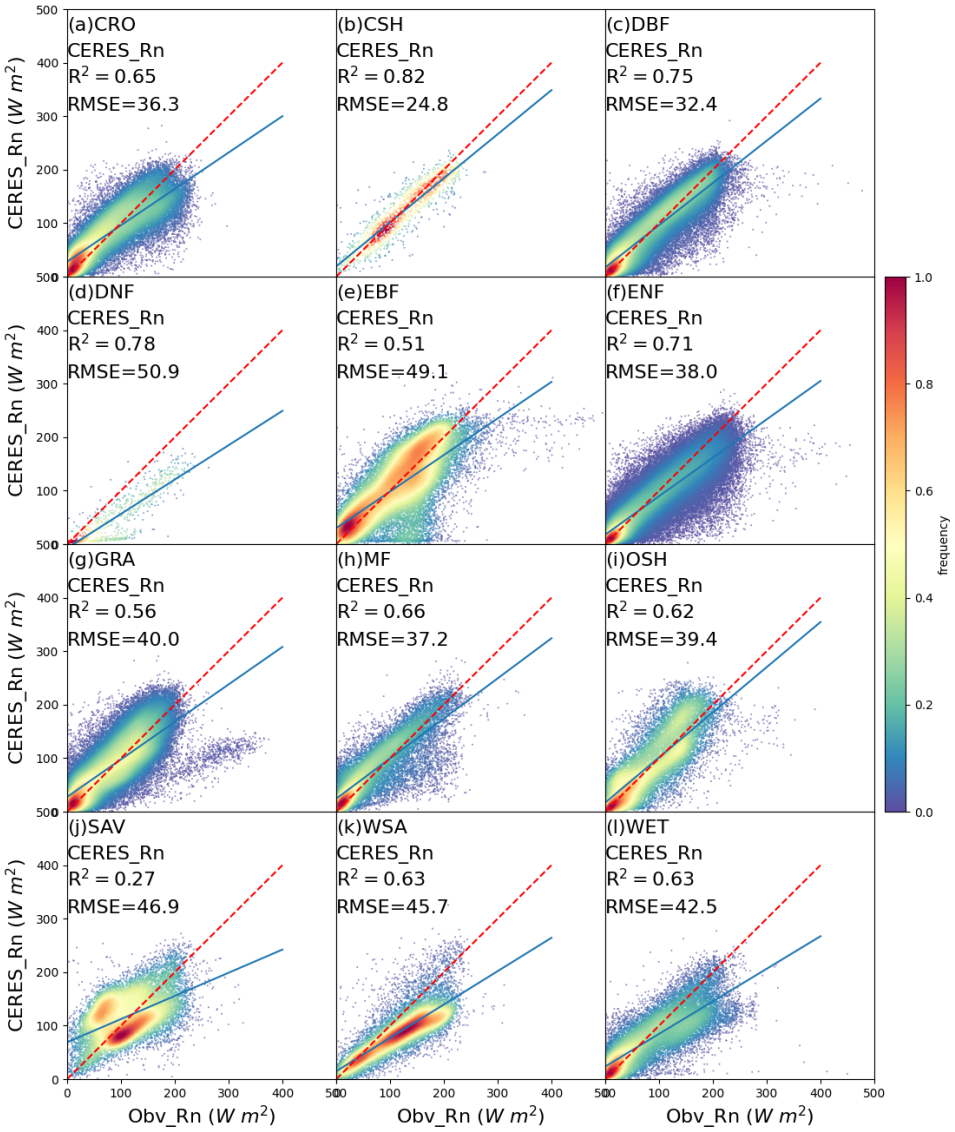

Figure S2. The scatter plot of daily net radiation from CERES (CERES_Rn) with the Rd from CERES as inputs compared with local instruments measurements (Obv_Rn) under 12 IGBP land cover types: CRO (Croplands), CSH (Closed shrublands), DBF (Deciduous broadleaf forests), DNF (Deciduous needle leaf forests), EBF (Evergreen broadleaf forests), ENF (Evergreen needle leaf forests), GRA (Grasslands), MF (Mixed forests), OSH (Open shrublands), SAV (Savannas), WSA (Woody savannas), WET (Permanent wetlands). The red dotted line is the 1:1 line. R is correlation coefficients, RMSE is Root Mean Square Error. The frequency denotes the probability density estimated through the Kernel Density Estimation, KDE method with a Gaussian kernel, and it is then scaled to ensure that the maximum value of the probability density function equals 1.

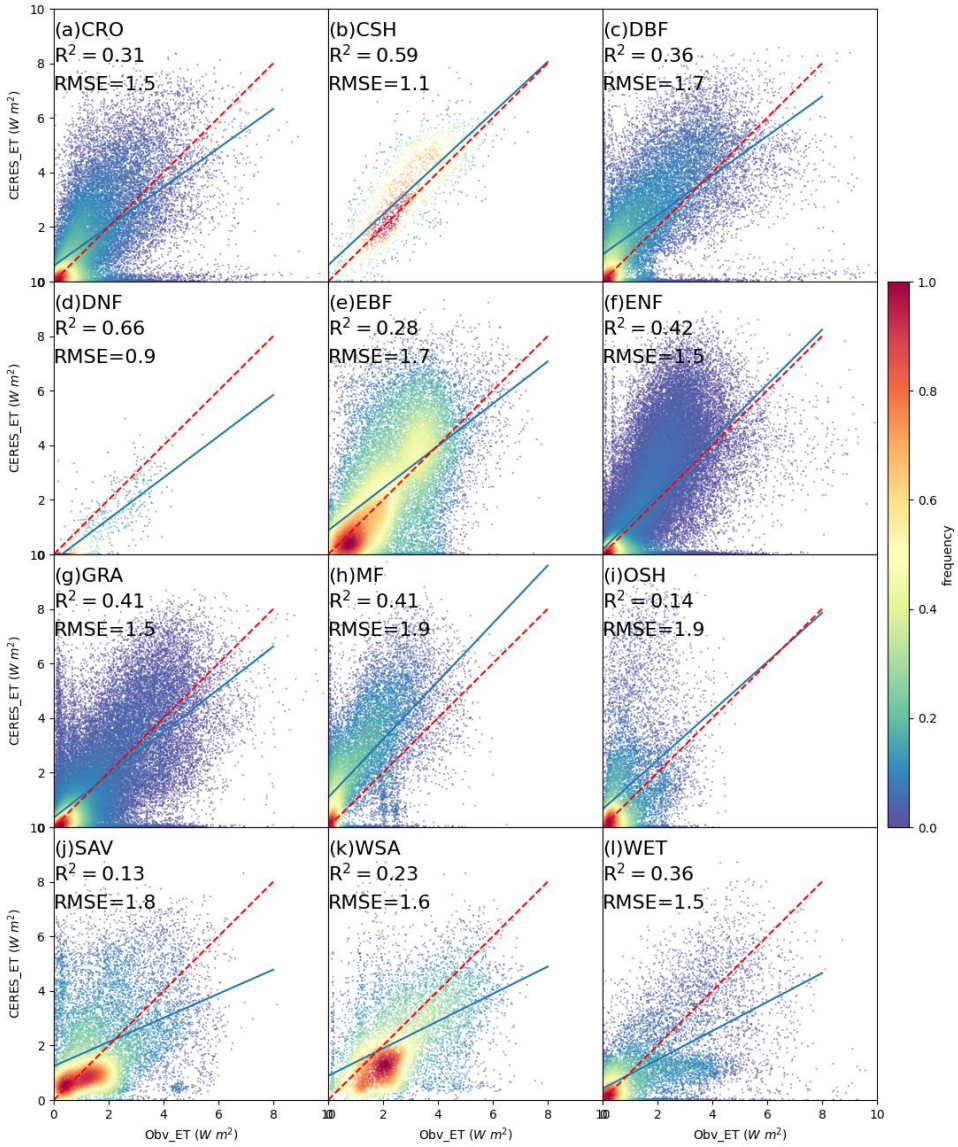

Figure S3. The scatter plot of daily ET simulated by VISEA (VISEA_Rn) with the Rd from CERES as inputs compared with local instruments measurements (Obv_Rn) under 12 IGBP land cover types: CRO (Croplands), CSH (Closed shrublands), DBF (Deciduous broadleaf forests), DNF (Deciduous needle leaf forests), EBF (Evergreen broadleaf forests), ENF (Evergreen needle leaf forests), GRA (Grasslands), MF (Mixed forests), OSH (Open shrublands), SAV (Savannas), WSA (Woody savannas), WET (Permanent wetlands). The red dotted line is the 1:1 line. N is the number of data points, NSE is Nash-Sutcliffe Efficiency, R is correlation coefficients, RMSE is Root Mean Square Error, RMSEs is systematic RMSE, and RMSEu is unsystematic RMSE. The frequency denotes the probability density estimated through the Kernel Density Estimation, KDE method with a Gaussian kernel, and it is then scaled to ensure that the maximum value of the probability density function equals 1.

The EF calculation based on the Ts-VI method requires local meteorological parameters for converting instantaneous EF into daily scale. Alternatively, directly using the instantaneous EF as its daily mean value can result in a 10% - 30% underestimation of daily ET. However, the challenge arises when attempting to calculate EF on a global scale and in near-real-time, as acquiring these local meteorological parameters globally and promptly is a formidable task.

As mentioned in lines 259-261, "However, some studies have found that the VI-Ts method may not consistently provide satisfactory results, especially in colder regions where vegetation thrives better under higher temperatures."

Furthermore, as highlighted in lines 653 – 657, "… in regions where the vegetation index and temperature data in adjacent grid cells show small variations, such as dense forests and bare lands and deserts. Also, in regions with freezing temperatures, the VI-TS method does perform well, because warmer temperature is related to increased vegetation, opposite the other regions, where there is a positive correlation between the vegetation index and surface temperature (Cui et al., 2021)."

What is the differences of this data product with other global ET on the long-term trend, inter-annual variation, and under extreme climate events?

Re: We have added long-term trends and inter-annual variations for these ET products in Figure 8 and we added the description about the long-term trend, inter annual variation at Lines 554-556:
"The VISEA ET product demonstrates consistent spatial distribution patterns among the six ET products across various years, both in terms of annual means (a-g) and latitude zonal means (h). These patterns align closely with the precipitation distribution data from GPCC."

And Lines 583-588 "Regarding the inter-annual monthly variations, panel (i) shows the fluctuations in ET across different years for the analyzed ET products and precipitation data. The graph reveals a rhythmic pattern of ET across the years, VISEA with other ET products showed distinctive peaks and troughs that correspond to seasonal changes and inter-annual climate variability. The ET products' data exhibit a close

alignment with the precipitation patterns reported by GPCC, highlighting the interconnectedness between ET and precipitation as climatic variables."

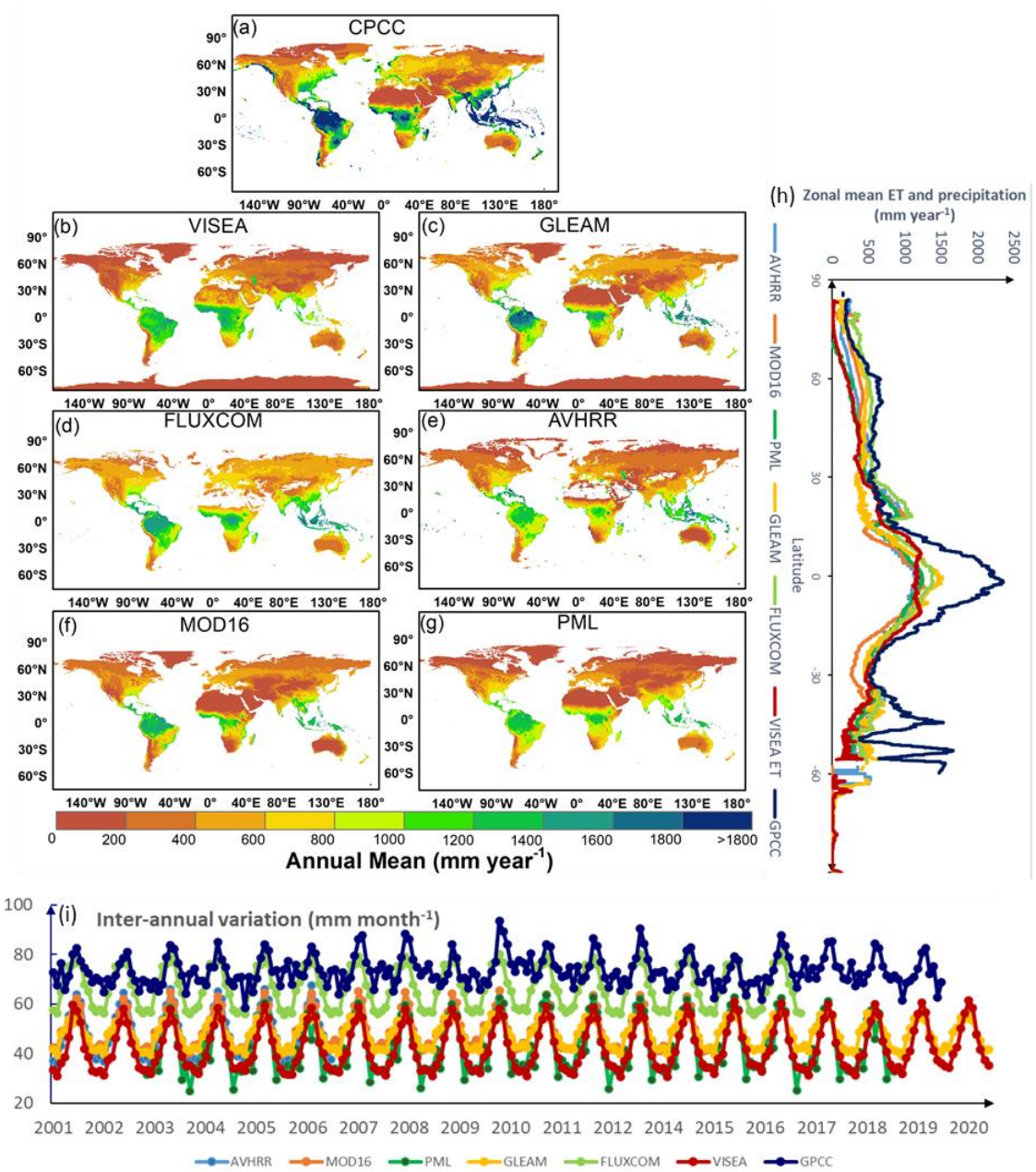

Figure 8. The spatial distribution of the multi-year average (a-g), the zonal mean (h) and inter-annual variation (i) of (a) GPCC (2001-2019), (b) VISEA (2001-2020), (c) GLEAM (2001-2020), (d) FLUXCOM (2001-2016), (e) AVHRR (2001-2006), (f) MOD16 (2001-2014) and (g) PML (2003-2018).

To demonstrate the performance of our data product under extreme climate conditions, we have added the 5th and 95th percentage spatial patterns in Supplementary Figure S1 and Figure S2. At lines 586-588: "It also exhibits similar distributions to other ET products, both below the 5th percentile (Figure S4) and above the 95th percentile (Figure S5)."

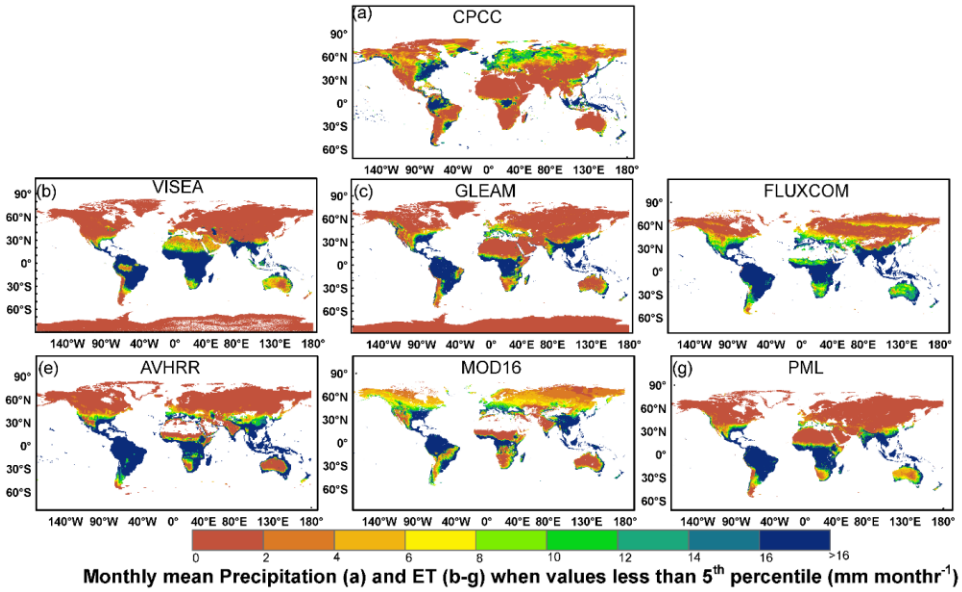

Figure S4. Monthly mean precipitation (a) and ET (b-g) when values less than 5th percentile (mm month^{-1}) (a) GPCC (2001-2019), (b) VISEA (2001-2020), (c) GLEAM (2001-2020), (d) FLUXCOM (2001-2016), (e) AVHRR (2001-2006), (f) MOD16 (2001-2014) and (g) PML (2003-2018).

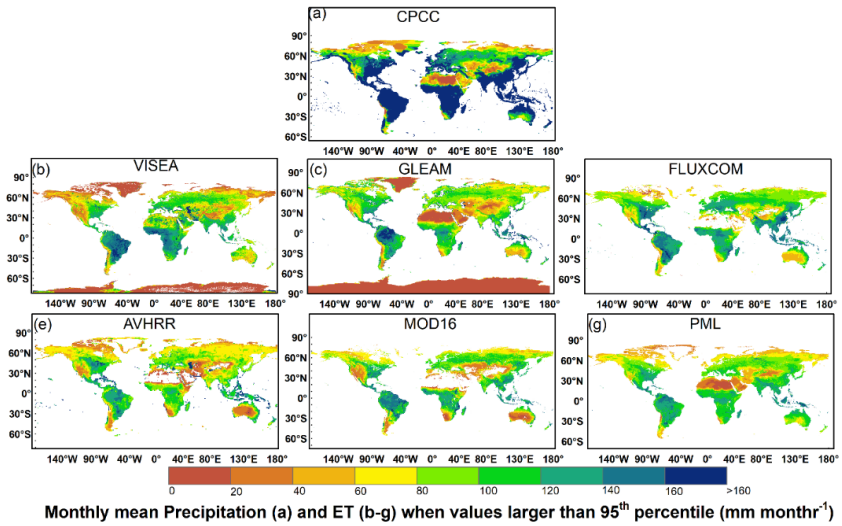

Figure S5. Monthly mean precipitation (a) and ET (b-g) when values large than 95th percentile (mm month^{-1}) (a) GPCC (2001-2019), (b) VISEA (2001-2020), (c) GLEAM (2001-2020), (d) FLUXCOM (2001-2016), (e) AVHRR (2001-2006), (f) MOD16 (2001-2014) and (g) PML (2003-2018).

Line 228: correct the label for surface temperature.

Re: We have corrected the label for surface temperature at Lines 226:

"2.1.3 The calculation of daily air temperature, T_a^d and surface temperature, T_s^d"

L118-120: this description seems not correct since VISEA also use the thermal information such as surface temperature.

Re: we modified this sentence at line 143 – 145:

"Unlike energy budget-based ET algorithms (such as SEBS, METRIC, and Alexi), which calculate ET (latent heat flux) as the residual of the net radiation, subtracting soil heat flux and sensible heat flux."

L209-216: how Ta is estimated for each 0.05 degree pixel?

Re: we explain the calculation progress of air temperature at lines 231-237:

"This method was developed based on the empirical linear relationship between surface temperature (Ts) and Vegetation Index (VI). Surface temperature increases when the vegetation index decreases, and conversely, surface temperature decreases when the vegetation index increases. By defining a "window" formed by the neighboring 5 * 5 grid cells, the scatter plot of these 25 grid cells' VI and Ts typically exhibits a triangular (or trapezoidal) distribution. In this scatter plot, we identify the "warm edge" (characterized by a low vegetation cover fraction and high Ts) and the "cold edge" (marked by a high vegetation cover fraction and low Ts).

Through simple interpolation, Ts corresponding to any given vegetation condition within the range of the "warm edge" and "cold edge" can be determined. The lowest Ts could be determined by the highest VI,

and the highest Ts could be determined by the lowest VI. Therefore, following Nishida et al. (2003), under the assumption that the lowest surface temperature equals the air temperature (Ta), we can derive the daily air temperature."

L238-246: how is air temperature of each pixel estimated?

Re: we explained the calculation progress at lines 231-237 above.

L297-301: rephrase.

Re: we have rephrased this sentence at lines 308-310:
"We evaluated the accuracy of the input ERA5-Land shortwave radiation, estimated daily net radiation, air temperature, and ET by comparing them against measurements from FLUXNET2015 (Pastorello et al., 2020). The data from FLUXNET2015 can be obtained at https://fluxnet.org/data/download-data."

L390-399: confusing on the differences between Ts and Ta.

Re: we explained at line 168: "*Ts*, land surface temperature" and at lines 32: "…air temperature (Ta)."

Figs 3-6: explain what frequency mean.

Re: we added the explanation of "frequency" at Figure 3- Figure 6:

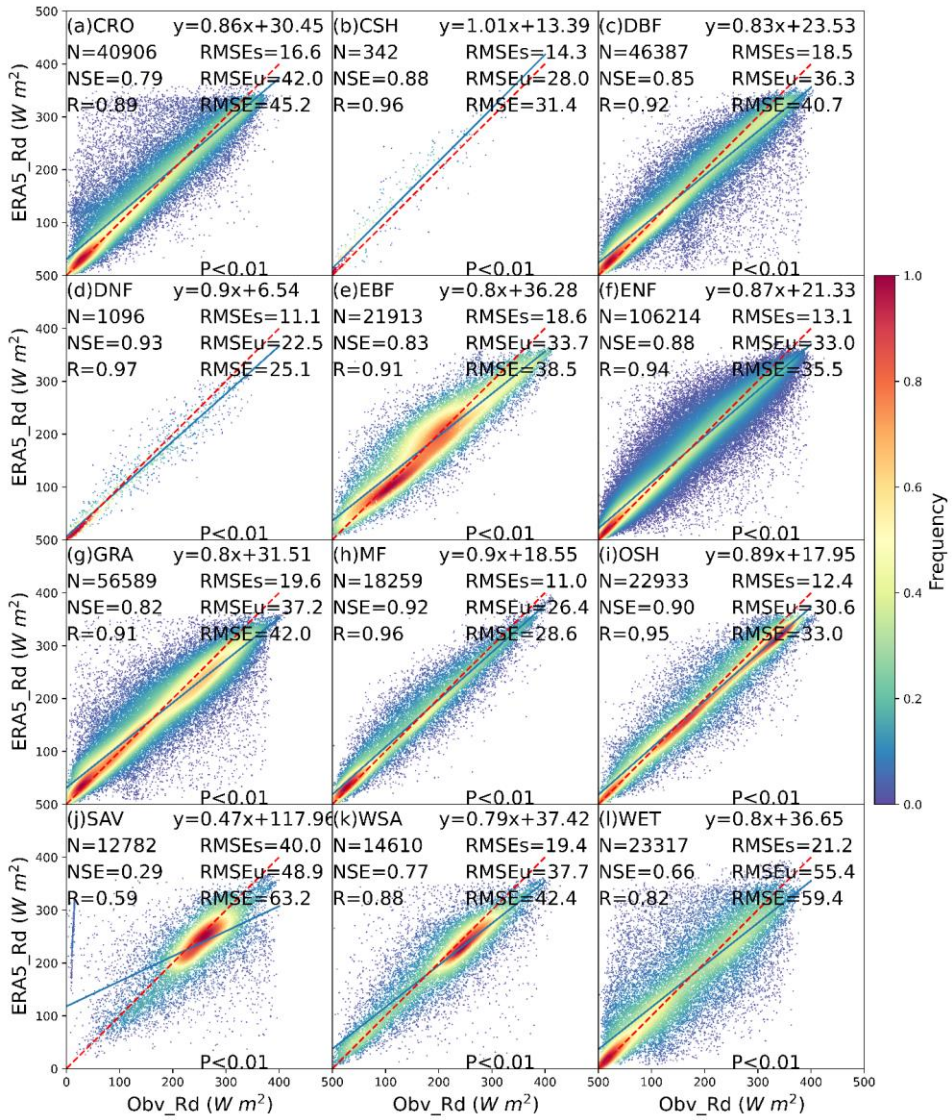

Figure 3. The scatter plot of downward solar radiation from ERA5-Land (ERA5_Rd) compared with local instruments measurements (Obv_Rd) under 12 IGBP land cover types: CRO (Croplands), CSH (Closed shrublands), DBF (Deciduous broadleaf forests), DNF (Deciduous needle leaf forests), EBF (Evergreen broadleaf forests), ENF (Evergreen needle leaf forests), GRA (Grasslands), MF (Mixed forests), OSH (Open shrublands), SAV (Savannas), WSA (Woody savannas), WET (Permanent wetlands). The red dotted line is the 1:1 line. N is the number of data points, NSE is Nash-Sutcliffe Efficiency, R is correlation coefficients, RMSE is Root Mean Square Error, RMSEs is systematic RMSE, and RMSEu is unsystematic RMSE. The Frequency denotes the probability density estimated through the KDE method with a Gaussian kernel, and it is then scaled to ensure that the maximum value of the probability density function equals 1. P is the P-Value for the Correlation Coefficient.

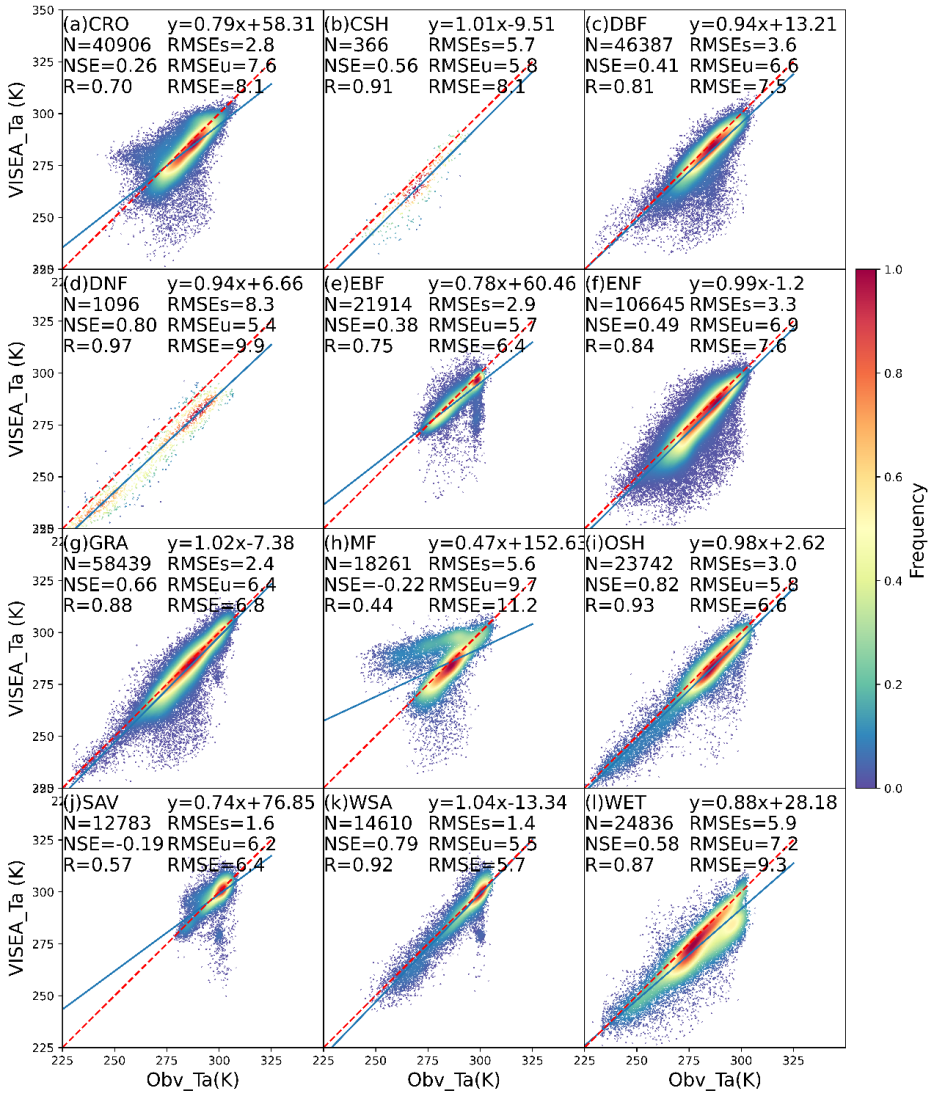

Figure 4. The scatter plot of daily air temperature simulated by VISEA (VISEA_Ta) compared with local instruments measurements (Obv_Ta) under 12 IGBP land cover types: CRO (Croplands), CSH (Closed shrublands), DBF (Deciduous broadleaf forests), DNF (Deciduous needle leaf forests), EBF (Evergreen broadleaf forests), ENF (Evergreen needle leaf forests), GRA (Grasslands), MF (Mixed forests), OSH (Open shrublands), SAV (Savannas), WSA (Woody savannas), WET (Permanent wetlands). The red dotted line is the 1:1 line. N is the number of data points, NSE is Nash-Sutcliffe Efficiency, R is correlation coefficients, RMSE is Root Mean Square Error, RMSEs is systematic RMSE, and RMSEu is unsystematic RMSE. The frequency denotes the probability density estimated through the Kernel Density Estimation, KDE method with a Gaussian kernel, and it is then scaled to ensure that the maximum value of the probability density function equals 1.

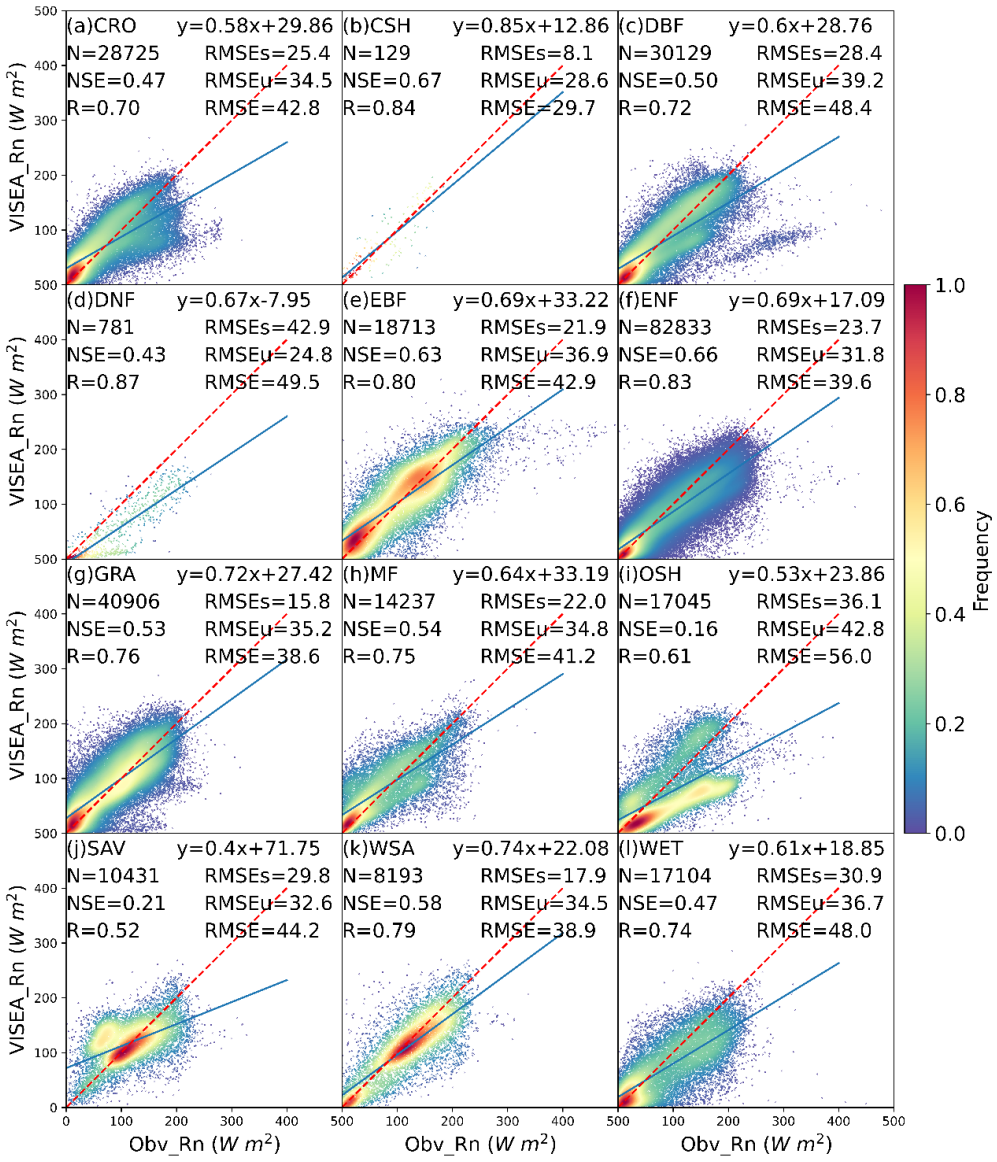

Figure 5. The scatter plot of daily net radiation simulated by VISEA (VISEA_Rn) compared with local instruments measurements (Obv_Rn) under 12 IGBP land cover types: CRO (Croplands), CSH (Closed shrublands), DBF (Deciduous broadleaf forests), DNF (Deciduous needle leaf forests), EBF (Evergreen broadleaf forests), ENF (Evergreen needle leaf forests), GRA (Grasslands), MF (Mixed forests), OSH (Open shrublands), SAV (Savannas), WSA (Woody savannas), WET (Permanent wetlands). The red dotted line is the 1:1 line. N is the number of data points, NSE is Nash-Sutcliffe Efficiency, R is correlation coefficients, RMSE is Root Mean Square Error, RMSEs is systematic RMSE, and RMSEu is unsystematic RMSE. The frequency denotes the probability density estimated through the Kernel Density Estimation, KDE method with a Gaussian kernel, and it is then scaled to ensure that the maximum value of the probability density function equals 1.

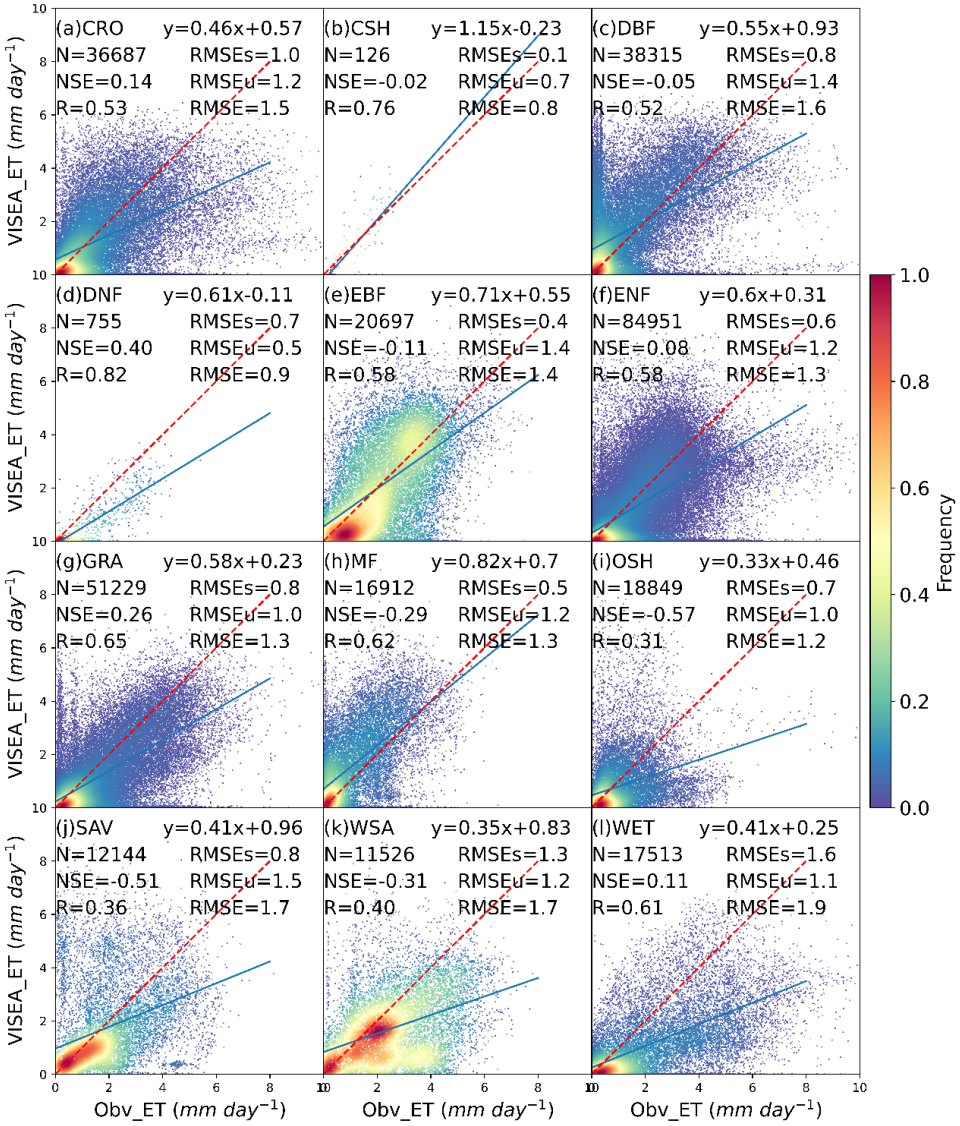

Figure 6. The scatter plot of daily ET simulated by VISEA (VISEA_ET) compared with local instruments measurements (Obv_ET) under 12 IGBP land cover types: CRO (Croplands), CSH (Closed shrublands), DBF (Deciduous broadleaf forests), DNF (Deciduous needle leaf forests), EBF (Evergreen broadleaf forests), ENF (Evergreen needle leaf forests), GRA (Grasslands), MF (Mixed forests), OSH (Open shrublands), SAV (Savannas), WSA (Woody savannas), WET (Permanent wetlands). The red dotted line is the 1:1 line. N is the number of data points, NSE is Nash-Sutcliffe Efficiency, R is correlation coefficients, RMSE is Root Mean Square Error, RMSEs is systematic RMSE, and RMSEu is unsystematic RMSE. The frequency denotes the probability density estimated through the Kernel Density Estimation, KDE method with a Gaussian kernel, and it is then scaled to ensure that the maximum value of the probability density function equals 1.

Figure 8: suggest adding a plot to show the global annual ET during the study period from these various data products.

Re: We have added a plot to show the global annual ET during the study period at Figure 8 before.

L515-529: need more precised description. Is there no regions with energy limited ET? Should be better to describe the differences in regions with moisture and energy limited ET.

Re: we added more precise description at lines 559-566:

"The available water for evaporation and transpiration is abundant, and the primary constraint on evapotranspiration lies in the availability of energy to drive the process. In such conditions, water availability is not a limiting factor, allowing for ample potential evapotranspiration."

We also added more precise description at lines 573-575:

"In these areas, there is a surplus of available energy, and the primary limitation on ET stems from the availability of water. This implies a high atmospheric water demand, often quantified as potential evapotranspiration (potential ET)."

We added the describe the differences in regions with moisture and energy limited ET at lines 576-582:

"In regions with moisture-limited evapotranspiration (ET), the primary constraint on ET arises from the limited availability of water. These areas typically experience insufficient precipitation or water supply, leading to a situation where the atmospheric demand for moisture exceeds the available water resources. On the other hand, regions with energy-limited ET face limitations due to inadequate energy for the process of evaporation and transpiration. This can be influenced by factors such as cloud cover, shading, or other conditions that limit the absorption of solar radiation. In such areas, even if there is an ample water supply, the lack of sufficient energy hinders the rate of evapotranspiration."

L530-546: can other global data product reveal the same pattern? Also need adding the conditions before 8/27/2022 to support the point that estimated ET could represent the soil moisture condition. Need clearly highlight the points for introducing this case analysis.

Re: We have incorporated daily scale GLEAM ET and CPC precipitation data from August 26th, 2022, which precedes the specified date of August 28, 2022. But we found GLEAM failed to capture the variability of ET during this drought and exhibited a negative correlation with precipitation data from CPC, so we wouldn't discuss it further in this context. And we added more description of Figure 9 at lines 602-612:

"VISEA ET graphically illustrates the evolving drought conditions: with notably low ET levels (below 1 mm day^{-1}) across the basin on August 26th to 28th, evidenced in panel (a-c). A notable increase in precipitation on August 29th, reflected in panels (s) and (u), correlates with an upswing in ET values (surpassing 1 mm day^{-1}) throughout the basin, as visualized in panels (d-f). The graph in panel (y) displays the variances in mean ET and precipitation within the basin over this timeframe, highlighting a significant rise in ET (up to 11 mm day^{-1}) on August 30th, which corresponds with the observed increase precipitation (reaching 11 mm day^{-1}) on August 29th.

VISEA's ET data align closely with the variances observed in the CPC precipitation data, showcasing its effectiveness in capturing daily ET fluctuations, especially during and after the drought conditions. It accurately reflects the dip and subsequent recovery in ET values following the precipitation events, indicating its robustness in near-real-time monitoring of ET during such hydrological extremes."

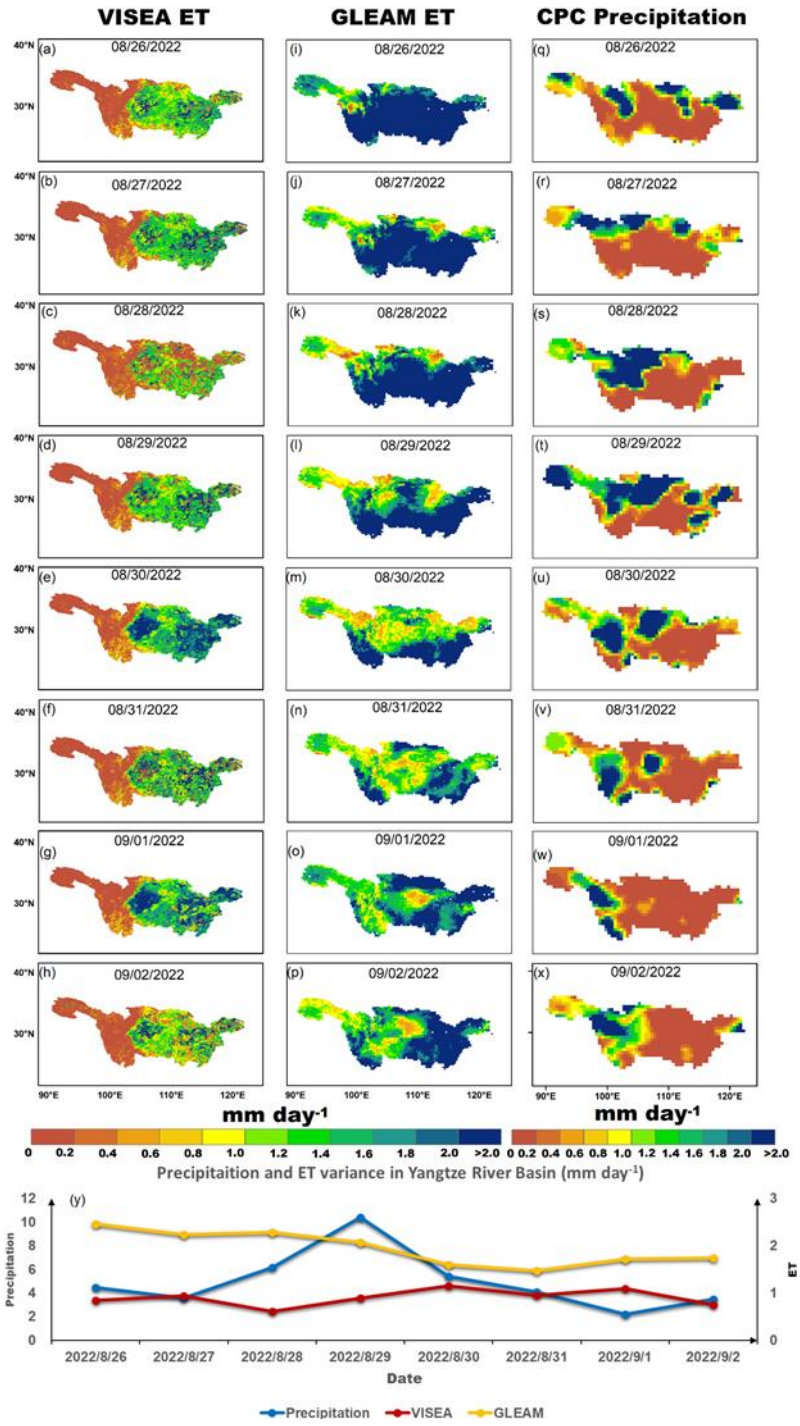

Figure 9. Daily ET from VISEA (a-h), GLEAM (i-p), and Precipitation (q-x) distributions from August 25th to September 2nd in 2022, alongside daily mean ET and Precipitation variances in the Yangtze River Basin (y) during the same period.

L579-582: It is confusing.

Re: we explained at lines 650-653:

"As previously explained, the VI-Ts method relies on the negative linear correlation between the Vegetation Index (VI) and surface temperature (Ts) within a 5 × 5 grid. Therefore, both the variance of VI values across these grid cells and the negative correlation are essential for calculating the air temperature."

L584: are you talking about the estimated air temperature?

Re: yes, in this paragraph, we are talking about the uncertainties of using VI-T_S method to calculate air temperature.

L586-587: should be more specific. What does "VISEA relies solely on vegetation coverage as an indirect constraint" mean?

Re: we added more specific description at lines 658-666:

"Another bias source of the VISEA model is the uncertainties of daily net radiation, notably originating from input downward shortwave radiation from ERA5-Land (Figure 2) and VI-Ts estimated air temperature (Figure 4). The energy budget equation (Eq. 11) and these two figures indicate that net radiation shows more uncertainties than shortwave radiation and air temperature. At the same time, assuming a linear relationship between cloud coverage (Eq. 12 and 13) and the calculation of downwards longwave radiation (Eq. 14 and 15) may be an oversimplification that could introduce uncertainties. Since available energy for evapotranspiration (ET) depends on net radiation (Eq. 16 and 17), addressing these uncertainties is crucial for enhancing overall model accuracy (Brutsaert, 1975; Huang et al., 2023). Future refinements will contribute to a more precise daily net radiation estimation within the VISEA model."

L604-605: where this conclusion come from?

Re: We modified this conclusion at lines 727-728:

"It demonstrates competitive correlation coefficients and Nash-Sutcliffe efficiencies (NSEs) across most land cover types but exhibits higher biases."

L607-608: the claim that "VISEA aligns with GPCC a... in most areas worldwide" is confusing. Does VISEA generate precipitation?

Re: we revised this sentence at lines 730-734:

"VISEA consistently demonstrates spatial patterns aligned with GPCC in most areas, featuring elevated values in tropical rainforest regions and lower values in arid and semi-arid zones. This alignment underscores VISEA's proficiency in portraying the spatial distribution of evapotranspiration, offering valuable insights into water consumption dynamics across diverse geographical regions."

L668-670: add more literature to support this claim. Why are the effects of VPD and leaf water potential on canopy surface resistance so minor that it could be removed totally in the equation?

Re: we have added more literature to support this claim at Lines 845-850:

"Tang et al. (2009) employed this canopy resistance approach to estimate evapotranspiration (ET) at a 500 meter resolution in the Kalam river basin. The evaluation of their results indicated that the simplification of these calculations did not significantly impact the final accuracy of ET estimates. Additionally, Huang et al. (2017, 2021, and 2023) evaluated this method for 0.05 degree ET assessments across China. The evaluation results also demonstrated that the reduction in vapor pressure deficit (VPD) and leaf water potential had minimal effects on the final ET estimates."